Adaptive Predictor-Feedback Control of SIRD Epidemiological Model with Uncertain Parameters and Input Delay

Author
Nikolaos Intas

Supervising Professor
Nikolaos Bekiaris-Liberis

Thesis Review Committee
Nikolaos Bekiaris-Liberis
Nikolaos Giatrakos
Florent Koudohode

Department of Electrical & Computer Engineering
May 2025

Acknowledgments

The cycle of my undergraduate studies is finally reaching its conclusion. It has been a fulfilling journey, marked by adventures, challenges and accomplishments. During this journey, I had the pleasure to meet exceptional and accomplished individuals - students, professors and associate staff alike. I was able to familiarize myself with various areas of electrical computer engineering, on both a theoretical and hands-on level. But most importantly, I was given the opportunity to expose myself to the world and build a solid foundation of problem-solving-oriented thinking that will accompany me throughout life.

First and foremost, I would like to thank my supervisor, Professor Nikolaos-Bekiaris Liberis, for trusting me with the subject of this thesis, as well as providing me with the direction required to successfully carry through with this task. I would also like to thank the members of the Thesis Review Committee, Professor Nikolaos Giatrakos and Dr. Florent Koudohode for devoting their time in assessing this thesis and providing valuable feedback to my work.

Additionally, I would like to thank the entirety of the Technical University of Crete staff, including professors, lab directors, assistants and administration personnel. The cumulative effort these individuals keeps the organization running, enabling students to achieve their intellectual potential and create credible academic work in all areas of engineering.

Last but not least, I would like to express my deepest gratitude to all members of my family for helping me reach this first milestone in my academic expedition. Despite the daily challenges and struggles, especially during the COVID-19 pandemic, they were able to aid me with every means in their disposal so I can achieve my academic goals. I would have never made it this far without you.

Abstract

In this thesis, we present an adaptive predictor-feedback controller for the widely-used $SIRD$ epidemiological model. The behavior of systems such as the $SIRD$ model is usually influenced by parameter uncertainty as well as various time delays which manifest in the system's dynamics. The control law proposed in this work aims to compensate for both of these phenomena while ensuring the stability of the system.

Chapter 1 serves as the introduction to our work. The recent COVID-19 pandemic functions as the primary motivating factor behind this thesis. We initially discuss the characteristics of the disease, as well as the effects of the pandemic as a whole. Then, we expand on the scientific field of mathematical epidemiology and provide various examples of models used in its study. We focus on compartmental models and draw comparisons to other popular modeling methods, such as agent-based models.

In Chapter 2, we focus on the mathematical analysis of the proposed model. In the beginning, we present the baseline $SIRD$ model as well as some important assumptions about the system's behavior. Then, we gradually present various control laws to compensate for the system's parameter uncertainty and time delays, as well as provide the mathematical foundations for the simulations used in the next chapter.

In Chapter 3, we present the simulation results of our proposed control law implementations for various different adaptation gain and constant values. We then discuss the effects of these parameter values in the system's behavior, as well as compare the simulation results between control law implementations.

Chapter 4 serves as the conclusion to this thesis. We briefly discuss the key takeaways of our work, alternative approaches, as well as various ways that we could possibly expand on it in the future.

Contents

Chapter 1

Introduction

1.1 The COVID-19 Pandemic

A population's health is of paramount importance to societal progress. Combating the stress induced by health-related factors enables individuals to grow and prosper. Prosperity on an individual level directly correlates to broader development, as a healthy society is far more likely to experience economic growth and, subsequently, better living standards [1]. Despite recent breakthroughs in both medicine and technology, factors such as communicable diseases can directly undermine these advancements.

Communicable disease outbreaks can vary a lot in the way they manifest. A disease can be highly deadly, but have very profound symptoms and be transmissible in a predictable way. This means that cases of infected individuals can be easily identified and isolated, rendering the reproductive rate of the disease relatively controllable. A good example of this are the periodic outbreaks of Ebola virus that have occurred since 1976 up to present day [2].

Other types of communicable diseases spread unpredictably, as individuals might experience highly varied symptoms between one another, or, in some cases, no symptoms at all. This makes tracking down and isolating cases of infected individuals in a timely manner a strenuous task. The outbreak of such a disease can prove quite difficult to contain. This is a common occurrence with diseases that target the respiratory system. Recent examples include the 2002-2004 SARS outbreak [3] and, more recently and on a much larger scale, the COVID-19 pandemic.

1.1.1 Overview of COVID-19

COVID-19 is a communicable disease caused by severe acute respiratory syndrome coronavirus 2, or SARS-CoV-2 for short. The virus is primarily transmitted through respiratory droplets expelled by either the nose or the mouth of an infected individual [4], however airborne transmission through aerosol-generating procedures or contaminated surfaces has also been observed [5].

The effects of COVID-19 can vary greatly between infected individuals, from completely asymptomatic cases, to fever and mild respiratory symptoms, to even harsher symptoms such as severe pneumonia and hemoptysis [6]. Milder symptoms are experienced among younger individuals. The majority of severe cases which often result in hospitalization or even mortality, are made up of older adults, usually aged 65 or older [7], or individuals with preexisting conditions, such as cardiovascular and autoimmune diseases or obesity. As such, these groups are highlighted as the most vulnerable to the disease [8].

1.1.2 Course of the Pandemic

The first confirmed case of an individual infected with COVID-19 can be traced back to the city of Wuhan, China on December 8, 2019 [9]. Within the next few months, the disease quickly spread to the rest of the world, resulting in the World Health Organization declaring COVID-19 a public health emergency of international concern on January 30, 2020 and eventually characterizing it as a pandemic on March 30 of the same year [10]. International trade and air travel are considered the primary factors that contributed to the worldwide spread of the disease, as noted in European countries such as Italy, France as well as the USA [11].

The highly contagious nature of COVID-19 constituted governmental controls aiming to minimize strain on the public health system and mitigate the number of mortality cases. Countries that rapidly enforced quarantine policies during the initial stages of the pandemic suffered far fewer deaths in comparison to countries with similar health expenditure percentages that did not do so. Greece serves as a good example of this [12]. However, lockdown strategies have serious socioeconomic repercussions, rendering them unsustainable long-term. They best serve as a stopgap measure to control the disease outbreak or in conjunction with effective vaccination methods until herd immunity has been achieved [13].

An unprecedented initiative was taken to rapidly develop and deploy effective and safe for use vaccines against COVID-19. Emergency use authorization for several different vaccines was granted by the US Food and Drug Administration as well as the European Medicines Agency in late 2020 and early 2021 [14]. A worldwide vaccination campaign took off shortly after. The ability of the virus to rapidly mutate posed a significant challenge, as numerous variants emerged throughout the course of the pandemic, with the currently deployed vaccines having varying efficacy rates between said variants [15]. This meant that vaccine development had to be constantly reevaluated to compensate for the numerous viral mutations.

On May 5, 2023, more than 3 years after the initial outbreak, the World Health Organization finally established that COVID-19 no longer fit the definition of international public health emergency [10].

1.1.3 Aftermath and Key Takeaways

Despite the collective efforts of medical personnel worldwide, as of December 31, 2023, more than 7 million deaths have been cumulatively attributed to COVID-19 [16]. Furthermore, sectors such as the economy, mental health and education were also compromised by the pandemic. Even though the disease does not currently pose a threat to international health, the possibility of a new outbreak is still present. This necessitates the constant awareness of the health mechanisms in place.

In today's world, international trade and travel remain a vital necessity for a global economy. This means that if a new disease outbreak is not effectively contained, it can quickly escalate to a global health crisis, as was the case with COVID-19.

Health organizations and governments alike must remain vigilant and refine the rapid-response systems at their disposal in order to prevent similar outbreaks in the future. Conducting meta-analysis and research on published data through the construction of accurate epidemic models is the key to achieving these goals.

1.2 Mathematical Epidemiology

The purpose of mathematical epidemiology is to design a model that predicts the future behavior of a disease outbreak. What motivates this effort is the

development and deployment of efficient control policies, via vaccination or other means, in order to try and minimize the number of infections, strain on the public health system and, consecutively, the number of deaths in the affected population.

The first systematic effort to develop a mathematical model in regards to epidemiology can be traced back to Daniel Bernoulli in 1760. Bernoulli created a model with the purpose of assessing the long-term advantages of inoculating a population against smallpox, since a percentage of the population would likely perish during said inoculation [17]. The results of Bernoulli's work would serve as motivation for epidemiologists in the centuries to follow.

The two primary types of mathematical models currently used in epidemiology are compartmental models and agent-based models.

1.2.1 Compartmental Models

The predominant approach in describing the dynamics of a communicable disease within a population is by using a compartmental model. Compartmental models divide the population into groups based on the health status of each individual. The transition of individuals between groups, both qualitatively and quantitatively, is then described using mathematical equations. In the case of continuous time models, this is done using sets of ordinary or partial differential equations. In the case of discrete time models, this is done using difference equations.

Simpler compartmental models generally assume determinism in their parameters. However, certain epidemiological effects are better described using stochasticity. An example of this is the random pattern at which infectious individuals come into contact with others during a disease outbreak [18]. As such, compartmental models can be further divided into stochastic and deterministic.

Basic compartmental models were originally conceptualized in a series of papers by W.O. Kermack and A.G. McKendrick between 1927 and 1933 [19]. A special case of the model introduced in this series is the SIR model which is considered the most fundamental model in mathematical epidemiology. The SIR model divides the population intro three compartments - susceptible (S), infected (I) and recovered (R). The transition of the population between compartments is modeled using a set of three differential equations. Additionally, it does not account for parameter uncertainty. As such, the model

serves as a good example of a deterministic differential equation model. Its dynamics can be briefly described by the block diagram shown in Figure 1.1.

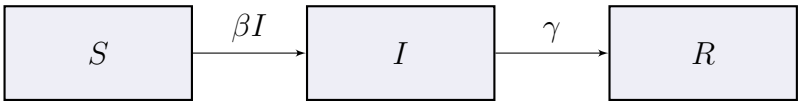

Figure 1.1: The block diagram of the SIR model. Parameters β and γ describe the transition rate of individuals between states.

Compartmental models are defined by their simplicity and intuitive structure. These benefits however come with the detriment of certain assumptions that might not entirely match real-world complexities. One such example is the assumed homogeneity of the subject population. Behavioral patterns as well as immune systems can vary greatly between individuals. Both of these factors can be detrimental to disease transmission, however they are very hard to describe using a compartmental model of reasonable complexity.

Despite their shortcomings, compartmental models comprise an invaluable epidemiological tool. They can easily adopt empirical data, which enables rapid policy adjustment, as well as useful meta-analysis. Their flexibility allows the modeling of a very broad range of varying disease dynamics. Strong mathematical tools such control theory can also be applied, encouraging a multitude of different approaches to the same epidemiological scenario. A few examples of commonly used compartmental models are presented below:

- SIR: The most fundamental epidemiological model. It aggregates the model population into three different groups - susceptible (S), infectious (I) and recovered (R). Recovered individuals are usually considered to have achieved permanent immunity. Used in bibliography to model the dynamics of diseases such as influenza [20], COVID-19 [21] and smallpox [22].

- $SIRD$: Expands on the base SIR model by incorporating a state (D) to account for deceased individuals. Frequently used in bibliography to model the dynamics of diseases with considerable mortality rates, such as Ebola [23], COVID-19 [24] or even more complex dynamics, such as the co-infection of Tuberculosis and HIV [25].

- $SEIR$: Expands on the SIR model by incorporating a state for exposed but not yet infectious individuals (E) Used in bibliography to model diseases with notable viral incubation periods, such as COVID-19 [26].

It is apparent that the SIR model provides a solid epidemiological modeling foundation which can be augmented with additional states to more accurately describe the disease dynamics we wish to model.

1.2.2 Agent-Based Models

Recent advancements in computer processing power and machine learning have given rise to the development of agent-based models (ABMs). These models are comprised by entities known as agents and aim to simulate the effects derived by the traits and behavioral patterns displayed among them. Autonomous agents are abstract entities, characterized by a multitude of attributes relevant to the purpose of the model. These attributes allow us to properly aggregate the population and deduct useful results for the study of the simulated phenomenon [27].

ABMs have proven useful in many scientific fields, including epidemiology. Unlike compartmental models which generally assume a certain level of population homogeneity, ABMs allow us to describe the effects of an infectious disease outbreak among a highly heterogeneous population. Each individual can be accurately described using attributes that directly correlate to the disease dynamics, such as age, weight and/or social circles. In addition, they allow us to accurately simulate the effects of various interventions, such as local lockdowns and vaccination policies, as well as the dynamic response of individual agents to those measures [28].

The rich information provided by ABMs however comes at a cost. Computational requirements are greatly increased, making the analysis of ABMs more expensive than the respective analysis of compartmental models. As model complexity grows, linking the behavior of the model to its structure can prove quite challenging [29]. As such, understanding the areas where the agent-based approach offers additional insight becomes crucial in order to avoid pitfalls such as unnecessary model complexity or data misinterpretation.

When choosing whether to use a compartmental or agent-based model to describe an infectious disease outbreak, a strictly better choice does not exist. One has to take into account the broader context of the situation and evaluate their choice based on the benefits and downsides that each approach offers. As agent-based models cannot be described using sets of differential equations, they cannot be used in the field of control theory.

Chapter 2

Proposed Model Analysis

2.1 The Base Model

Our goal in this chapter is to model the disease dynamics of the total population function N: $\mathbb{R}_0^+ \to \mathbb{R}^+$. We consider $t = 0$ the moment when the first subset of individuals included in population N get infected.

Let us divide the population into the following discrete compartments:

- S: The subset of the population that is susceptible to the disease.
- I: The subset of the population that is infected by the disease.
- R: The subset of the population that has recovered from the disease.
- D: The subset of the population that has succumbed to the disease.

We can define functions S, I, R, D: $\mathbb{R}_0^+ \to \mathbb{R}_0^+$ in order to describe each of the aforementioned compartments. Since these functions describe the population of each respective compartment, their respective values can either positive be or zero. As such, these functions have been defined over a positive codomain that also includes zero. Function S reaching value zero means that no susceptible individuals remain in the population. Function I reaching zero value means that the disease no longer exists among individuals in the population. Functions R and D having zero value means that no individuals have recovered from or died due to the disease respectively.

Next, let us assume that the disease dynamics of the model change in finite time. This means that $N \in \mathcal{C}^1$ and that its derivative with respect to time $\dot{N}$ is bounded. This, in turn, implies that S, I, R, $D \in \mathcal{C}^1$ and their respective

derivatives are also bounded. Let us assume $a, b, t^* \in \mathbb{R}^+$ with $a < t^* < b$. Since $N \in \mathcal{C}^1$, by invoking the Mean Value Theorem, for $t \in (t^*, b)$ there exists $c \in (t^*, t)$ such that:

$$\dot{N}(c) = \frac{N(t) - N(t^*)}{t - t^*} \tag{2.1}$$

By solving for N, taking its absolute value and using the triangle inequality, we get:

$$|N(t)| = |N(t^*)| + |\dot{N}(c)||(t - t^*)| \leq |N(t^*)| + |\dot{N}(c)|(b - a) = M \tag{2.2}$$

where $M \in \mathbb{R}^+$. We can prove this holds true for all $t \in (a, t^*)$ in an identical manner. For $t = t^*$, the upper bound is M itself. As such, the population N is bounded for all $t \in \mathbb{R}^+$.

Having proven the system population is a positive finite value, we can now normalize each individual compartment with respect to it. As such, the relationship between the model compartments can be expressed as:

$$S(t) + I(t) + R(t) + D(t) = 1 \tag{2.3}$$

When defining the dynamics of SIR-like systems, it is common practice to take into account the rate at which individuals enter the system population via birth or immigration and the rate at which individuals are removed from the population due to natural mortality[ref here]. Individuals entering the population this way are immediately added to the susceptible compartment at a specific rate, while individuals exiting the population this way are removed from each compartment that does not represent disease-related mortality. This is done at a fixed rate, proportional to the compartment's magnitude [30]. With this approach in mind, let us now define the proposed system dynamics using the following set of differential equations:

$$\begin{aligned}
\dot{S}(t) &= \lambda - \beta S(t) I(t) - \mu S(t) \\
\dot{I}(t) &= \beta S(t) I(t) - \gamma I(t) - \delta I(t) - \mu I(t) \\
\dot{R}(t) &= \gamma I(t) - \mu R(t) \\
\dot{D}(t) &= \delta I(t)
\end{aligned} \tag{2.4}$$

It is made apparent that the system dynamics not only depend on the population of each compartment, but also on constants β, γ, δ, λ, $\mu \in (0, 1)$. These constants are normalized with respect to the total population N and are described as follows:

- β: The transmission rate of the disease from an infected individual to a susceptible individual.
- γ: The recovery rate of infected individuals.
- δ: The mortality rate of infected individuals.
- λ: The rate at which individuals are added to the total population through birth or immigration.
- μ: The rate at which individuals are removed from the total population due to mortality unrelated to the disease.

It is important to note that the model distinguishes between individuals that die due to being infected from the disease and individuals that die due to unrelated causes. Individuals that succumb to the disease enter compartment D from compartment I at a rate δ and stay in that compartment indefinitely. Individuals that die due to unrelated causes exit the model population at a rate μ from either compartment S, I or R.

The base model dynamics can be clearly observed in Figure 2.1.

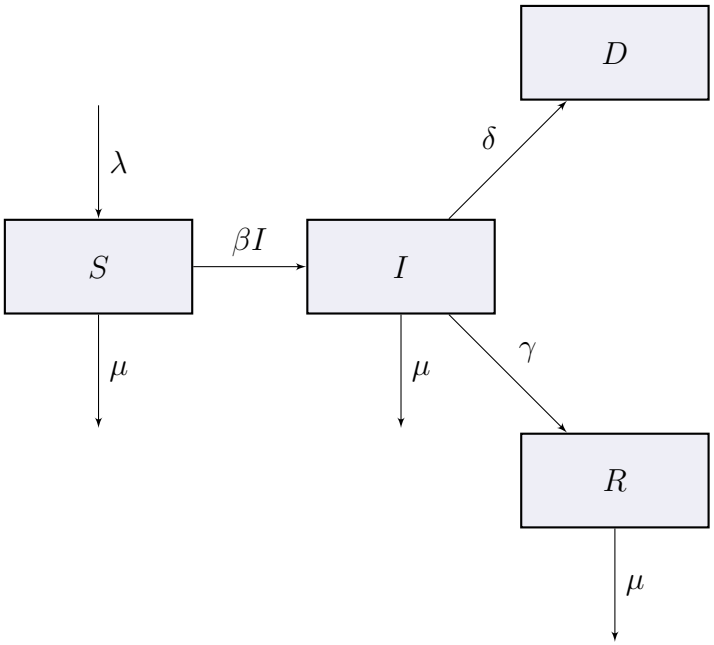

Figure 2.1: The block diagram of the proposed $SIRD$ model. Note the rate at which individuals enter and exit the total model population, as well as the rate at which individuals transition between compartments.

Let us define the state vector of the proposed system of differential equations $\mathbf{x}$: $\mathbb{R}_0^+ \to \mathbb{R}^4$ as:

$$\mathbf{x}(t) = \begin{bmatrix} S(t) \\ I(t) \\ R(t) \\ D(t) \end{bmatrix} \tag{2.5}$$

Since the values of the system compartments are normalized with respect to the total population N, we can obtain the initial conditions of the system as follows:

$$\mathbf{x}(0) = \begin{bmatrix} S(0) \\ I(0) \\ R(0) \\ D(0) \end{bmatrix} = \begin{bmatrix} 1 - \frac{n_0}{N(0)} \\ \frac{n_0}{N(0)} \\ 0 \\ 0 \end{bmatrix} \tag{2.6}$$

where n_0 is the total number of individuals that are initially infected and $N(0)$ is the initial value of the system's total population. We assume that no members of the population can immediately recover from or die due to the disease. As such, compartments R and D are initially empty. Our dynamical system can now be expressed as an initial value problem:

$$\dot{\mathbf{x}}(t) = f(\mathbf{x}(t)),\, \mathbf{x}(0)),\, \mathbf{x}(0) = \begin{bmatrix} 1 - \frac{n_0}{N(0)} & \frac{n_0}{N(0)} & 0 & 0 \end{bmatrix}^T \tag{2.7}$$

where f: $\mathbb{R}^4 \to \mathbb{R}^4$.

2.2 Uncertain Parameters and Adaptive Control Implementation

The behavior of dynamical systems can often become subject to the influence of uncertain parameters. This uncertainty is usually caused due to external factors, such as disturbances or noise, but it can also be inherent to the system dynamics by design. Such is the case with the $SIRD$ model, as the transition rates of individuals between compartments, as well as the rate at which they enter or exit the population are directly linked to a probability distribution.

In the version of the $SIRD$ model proposed in the previous section, these parameters are considered as known constants. By replacing these parameters with a known value (e.g. the expected value of the probability distribution), we can significantly simplify the analysis of our system. However, such a model design usually takes into account unrealistic assumptions about the

behavior of the system. In our case, the transition rates between compartments as well as the rate of change of the total population cannot be expected to be known and constant at all times, as they can drastically change over time.

It is helpful instead to consider those parameters as uncertain. Then, we can design a control law that adapts according to the behavior of the system over time and compensates for this uncertainty based on live parameter estimations. This approach in control design is known as Adaptive Control.

First, let us consider functions $\tilde{\beta}(t)$, $\tilde{\gamma}(t)$, $\tilde{\delta}(t)$, $\tilde{\lambda}(t)$, $\tilde{\mu}(t)$: $\mathbb{R}_0^+ \to [0,1]$ such that:

$$\begin{aligned}
\tilde{\beta}(t) &= \beta - \hat{\beta}(t) \\
\tilde{\gamma}(t) &= \gamma - \hat{\gamma}(t) \\
\tilde{\delta}(t) &= \delta - \hat{\delta}(t) \\
\tilde{\lambda}(t) &= \lambda - \hat{\lambda}(t) \\
\tilde{\mu}(t) &= \mu - \hat{\mu}(t)
\end{aligned} \tag{2.8}$$

where $\hat{\beta}$, $\hat{\gamma}$, $\hat{\delta}$, $\hat{\lambda}$ and $\hat{\mu}$ are estimates of the uncertain parameters β, γ, δ, λ and μ respectively. Additionally, let us assume that $\hat{\lambda}$, $\hat{\mu}$, $\hat{\beta}$, $\hat{\gamma}$, $\hat{\delta} \in \mathcal{C}^1$. This, in turn, implies that $\tilde{\beta}$, $\tilde{\gamma}$, $\tilde{\delta}$, $\tilde{\lambda}$, $\tilde{\mu} \in \mathcal{C}^1$. As such, the functions' derivatives with respect to time t can be consecutively obtained as:

$$\begin{aligned}
\dot{\tilde{\beta}}(t) &= -\dot{\hat{\beta}}(t) \\
\dot{\tilde{\gamma}}(t) &= -\dot{\hat{\gamma}}(t) \\
\dot{\tilde{\delta}}(t) &= -\dot{\hat{\delta}}(t) \\
\dot{\tilde{\lambda}}(t) &= -\dot{\hat{\lambda}}(t) \\
\dot{\tilde{\mu}}(t) &= -\dot{\hat{\mu}}(t)
\end{aligned} \tag{2.9}$$

Let us thus define an estimation vector $\mathbf{e}$: $\mathbb{R}_0^+ \to \mathbb{R}^5$ as:

$$\mathbf{e}(t) = \begin{bmatrix} \frac{1}{\sqrt{\alpha_1}}\tilde{\beta}(t) \\ \frac{1}{\sqrt{\alpha_2}}\tilde{\gamma}(t) \\ \frac{1}{\sqrt{\alpha_3}}\tilde{\delta}(t) \\ \frac{1}{\sqrt{\alpha_4}}\tilde{\lambda}(t) \\ \frac{1}{\sqrt{\alpha_5}}\tilde{\mu}(t) \end{bmatrix} = \begin{bmatrix} \frac{1}{\sqrt{\alpha_1}}(\beta - \hat{\beta}(t)) \\ \frac{1}{\sqrt{\alpha_2}}(\gamma - \hat{\gamma}(t)) \\ \frac{1}{\sqrt{\alpha_3}}(\delta - \hat{\delta}(t)) \\ \frac{1}{\sqrt{\alpha_4}}(\lambda - \hat{\lambda}(t)) \\ \frac{1}{\sqrt{\alpha_5}}(\mu - \hat{\mu}(t)) \end{bmatrix} \tag{2.10}$$

where parameters α_1, α_2, α_3, α_4, $\alpha_5 \in \mathbb{R}^+$ are considered known and called adaptation gains. Since all elements of vector $\mathbf{e}$ are $\mathcal{C}^1$, vector $\dot{\mathbf{e}}$ can be easily obtained as:

$$\dot{\mathbf{e}}(t) = \begin{bmatrix} \frac{1}{\sqrt{\alpha_1}}\dot{\tilde{\beta}}(t) \\ \frac{1}{\sqrt{\alpha_2}}\dot{\tilde{\gamma}}(t) \\ \frac{1}{\sqrt{\alpha_3}}\dot{\tilde{\delta}}(t) \\ \frac{1}{\sqrt{\alpha_4}}\dot{\tilde{\lambda}}(t) \\ \frac{1}{\sqrt{\alpha_5}}\dot{\tilde{\mu}}(t) \end{bmatrix} = \begin{bmatrix} -\frac{1}{\sqrt{\alpha_1}}\dot{\hat{\beta}}(t) \\ -\frac{1}{\sqrt{\alpha_2}}\dot{\hat{\gamma}}(t) \\ -\frac{1}{\sqrt{\alpha_3}}\dot{\hat{\delta}}(t) \\ -\frac{1}{\sqrt{\alpha_4}}\dot{\hat{\lambda}}(t) \\ -\frac{1}{\sqrt{\alpha_5}}\dot{\hat{\mu}}(t) \end{bmatrix} \tag{2.11}$$

Vector functions $\mathbf{e}$ and $\dot{\mathbf{e}}$ are going to be of great importance during the design process of the adaptive control law necessary to compensate for the uncertainty in the dynamics of the system.

In the context of the $SIRD$ model, we aim to regulate the rate at which susceptible individuals become infected, as well as the rate at which infected individuals recover from the disease or succumb to it. As such, let us introduce control inputs u_1, u_2, u_3: $\mathbb{R}_0^+ \to \mathbb{R}$ in a linear manner to compensate. These inputs represent the following:

- u_1: The implementation of social distancing and masking policies from non-infected but susceptible individuals.
- u_2: The implementation of isolation policies of currently infected individuals until recovery.
- u_3: The implementation of health-care processes, such as treatment and ICU infrastructure that impact the rate of recovery of infected individuals.

By considering constants $K_1, K_2, K_3 \in \mathbb{R}^+$, let us now define our adaptive control inputs as:

$$\begin{aligned} u_1(t) &= S(t)(\hat{\beta}(t)I(t) + \hat{\mu}(t) - K_1) - \hat{\lambda}(t) \\ u_2(t) &= I(t)(\hat{\gamma}(t) + \hat{\delta}(t) + \hat{\mu}(t) - \hat{\beta}(t)S(t) - K_2) \\ &\quad - \hat{\gamma}(t)R(t) - \hat{\delta}(t)D(t) \\ u_3(t) &= R(t)(\hat{\mu}(t) - K_3) \end{aligned} \tag{2.12}$$

Our closed-loop system now becomes:

$$\begin{aligned}
\dot{S}(t) &= \lambda - \beta S(t)I(t) - \mu S(t) + u_1(t) \\
\dot{I}(t) &= \beta S(t)I(t) - \gamma I(t) - \delta I(t) - \mu I(t) + u_2(t) \\
\dot{R}(t) &= \gamma I(t) - \mu R(t) + u_3(t) \\
\dot{D}(t) &= \delta I(t)
\end{aligned} \tag{2.13}$$

By defining an adaptive control law vector function $\mathbf{u}$: $\mathbb{R}_0^+ \to \mathbb{R}^4$ as:

$$\mathbf{u}(t) = \begin{bmatrix} u_1(t) \\ u_2(t) \\ u_3(t) \\ 0 \end{bmatrix} \tag{2.14}$$

we can rewrite our original system by defining function g: $\mathbb{R}^4 \times \mathbb{R}^4 \to \mathbb{R}$ as:

$$\dot{\mathbf{x}}(t) = g(\mathbf{x}(t), \mathbf{u}(t)) = f(\mathbf{x}(t)) + \mathbf{u}(t) \tag{2.15}$$

This choice of control law allows us to compensate for the uncertainty of parameters β, γ, δ, λ and μ while at the same time ensuring the stability of the closed-loop system. This is achieved by introducing the following Lyapunov candidate function V: $\mathbb{R}^4 \times \mathbb{R}^5 \to \mathbb{R}_0^+$ and $V \in \mathcal{C}^1$ with respect to time t and performing stability analysis using Lyapunov's direct method:

$$V(\mathbf{x}(t), \mathbf{e}(t)) = \frac{1}{2}||\mathbf{x}(t)||_2^2 + \frac{1}{2}||\mathbf{e}(t)||_2^2 \tag{2.16}$$

where $||\cdot||_2$ denotes the Euclidean norm. The function is obviously positive definite as the sum of squared factors. It's derivative $\dot{V}$ along the solutions of the system and the estimation vector yields:

$$\begin{aligned}
&\dot{V}(\mathbf{x}(t, \mathbf{e}(t))) = \mathbf{x}(t)\dot{\mathbf{x}}(t)^T + \mathbf{e}(t)\dot{\mathbf{e}}(t)^T \\
\Leftrightarrow\ &\dot{V}(\mathbf{x}(t), \mathbf{e}(t)) = S(t)\dot{S}(t) + I(t)\dot{I}(t) + R(t)\dot{R}(t) + D(t)\dot{D}(t) \\
&\qquad + \tilde{\beta}(t)\dot{\tilde{\beta}}(t) + \tilde{\gamma}(t)\dot{\tilde{\gamma}}(t) + \tilde{\delta}(t)\dot{\tilde{\delta}}(t) + \tilde{\lambda}(t)\dot{\tilde{\lambda}}(t) \\
&\qquad + \tilde{\mu}(t)\dot{\tilde{\mu}}(t)
\end{aligned} \tag{2.17}$$

Using the estimation vector components defined in (2.10) and (2.11), the derivative of the Lyapunov function candidate becomes:

$$\begin{aligned}
\dot{V}(\mathbf{x}(t), \mathbf{e}(t)) &= S(t)\dot{S}(t) + I(t)\dot{I}(t) + R(t)\dot{R}(t) + D(t)\dot{D}(t) \\
&\quad - \frac{1}{\alpha_1}(\beta - \hat{\beta}(t))\dot{\hat{\beta}}(t) - \frac{1}{\alpha_2}(\gamma - \hat{\gamma}(t))\dot{\hat{\gamma}}(t) \\
&\quad - \frac{1}{\alpha_3}(\delta - \hat{\delta}(t))\dot{\hat{\delta}}(t) - \frac{1}{\alpha_4}(\lambda - \hat{\lambda}(t))\dot{\hat{\lambda}}(t) \\
&\quad - \frac{1}{\alpha_5}(\mu - \hat{\mu}(t))\dot{\hat{\mu}}(t)
\end{aligned} \tag{2.18}$$

Using the equations of the closed-loop system defined in (2.13) and the adaptive control law defined in (2.12), the derivative of the Lyapunov function candidate now becomes:

$$\begin{aligned}
\Leftrightarrow \dot{V}(\mathbf{x}(t),\mathbf{e}(t)) &= S(t)((\lambda-\hat{\lambda}(t))+(\beta-\hat{\beta}(t))S(t)I(t)\\
&\quad-(\mu-\hat{\mu}(t))S(t)-K_1S(t))\\
&\quad+I(t)((\beta-\hat{\beta}(t))S(t)I(t)-(\gamma-\hat{\gamma}(t))I(t)\\
&\quad-(\delta-\hat{\delta}(t))I(t)-(\mu-\hat{\mu}(t))I(t)-K_2I(t))\\
&\quad+R(t)(\gamma-\hat{\gamma}(t))I(t)-(\mu-\hat{\mu}(t))R(t)-K_3R(t))\\
&\quad+D(t)(\delta-\hat{\delta}(t))I(t)-\frac{1}{\alpha_1}(\beta-\hat{\beta}(t))\dot{\hat{\beta}}(t)\\
&\quad-\frac{1}{\alpha_2}(\gamma-\hat{\gamma}(t))\dot{\hat{\gamma}}(t)-\frac{1}{\alpha_3}(\delta-\hat{\delta}(t))\dot{\hat{\delta}}(t)\\
&\quad-\frac{1}{\alpha_4}(\lambda-\hat{\lambda}(t))\dot{\hat{\lambda}}(t)-\frac{1}{\alpha_5}(\mu-\hat{\mu}(t))\dot{\hat{\mu}}(t)
\end{aligned} \tag{2.19}$$

At this stage it is impossible to guarantee the stability of the system, as the sign of our uncertain variables and, consecutively, the sign of the derivative of function V is unknown. In order to eliminate the effect of the uncertain parameters, we can define our parameter update laws as:

$$\begin{aligned}
\dot{\hat{\beta}}(t) &= \alpha_1 S(t)I(t)(I(t)-S(t))\\
\dot{\hat{\gamma}}(t) &= \alpha_2 I(t)(R(t)-I(t))\\
\dot{\hat{\delta}}(t) &= \alpha_3 I(t)(D(t)-I(t))\\
\dot{\hat{\lambda}}(t) &= \alpha_4 S(t)\\
\dot{\hat{\mu}}(t) &= -\alpha_5(S^2(t)+I^2(t)+R^2(t))
\end{aligned} \tag{2.20}$$

By using the parameter update laws defined in (2.20), the derivative of the Lyapunov function candidate becomes:

$$\begin{aligned}
\dot{V}(\mathbf{x}(t),\mathbf{e}(t)) &= (\beta-\hat{\beta}(t)-\beta+\hat{\beta}(t))S(t)I(t)(I(t)-S(t))\\
&\quad+(\gamma-\hat{\gamma}(t)-\gamma+\hat{\gamma}(t))I(t)(R(t)-I(t))\\
&\quad+(\delta-\hat{\delta}(t)-\delta+\hat{\delta}(t))I(t)(D(t)-I(t))\\
&\quad+(\lambda-\hat{\lambda}(t)-\lambda+\hat{\lambda}(t))S(t)\\
&\quad-(\mu-\hat{\mu}(t)-\mu+\hat{\mu}(t))(S^2(t)+I^2(t)+R^2(t))\\
&\quad-K_1S^2(t)-K_2I^2(t)-K_3R^2(t)\\
\Leftrightarrow \dot{V}(\mathbf{x}(t),\mathbf{e}(t)) &= -K_1S^2(t)-K_2I^2(t)-K_3R^2(t)
\end{aligned} \tag{2.21}$$

It is made apparent that the derivative is negative semi-definite. As such, we have successfully managed to design an adaptive control law that renders the closed-loop system stable in the sense of Lyapunov.

Let us also define the output vector of the closed loop system $\mathbf{y}$: $\mathbb{R}_0^+ \to \mathbb{R}^3$.

$$\mathbf{y}(t) = \begin{bmatrix} S(t) \\ I(t) \\ R(t) \end{bmatrix} \tag{2.22}$$

We will be measuring the behavior of the output vector during system simulations.

The closed-loop system's structure under adaptive control is presented thoroughly in the block diagram in Figure 2.2:

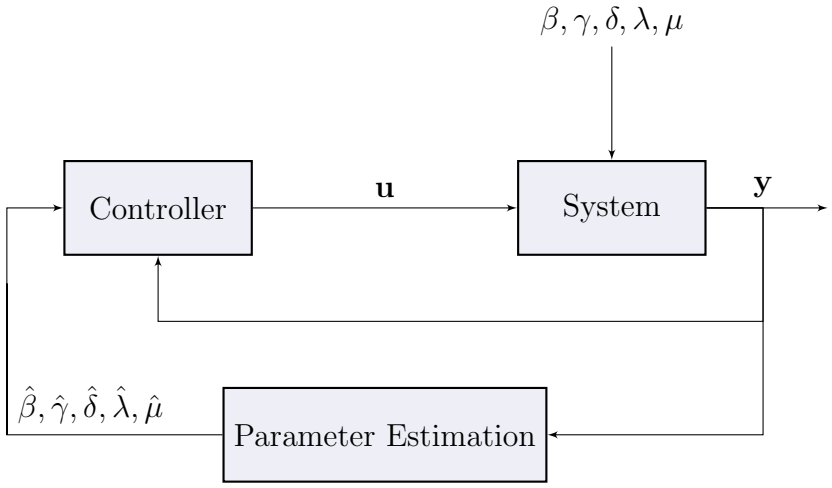

Figure 2.2: The block diagram of the closed-loop $SIRD$ model under adaptive control. Note how the system measurements are used in the calculation of the parameter estimations. The parameter estimations are then used in conjunction with the system measurements in the controller of the system.

2.3 Input Delay and Predictor-Feedback Control Implementation

When designing control laws for dynamical systems, we usually consider the ideal scenario where the controller can be updated with information from the system in real time. However, this is often not the case, as systems can become subject to various time delays. These delays can be attributed to a multitude of different factors. They usually present themselves directly in the state vector or the input of the control law that the system is subject to. In the context of the $SIRD$ model, this can be attributed to delayed detection of infected individuals, delayed population response to social distancing measures or other similar phenomena that the control law is attempting to emulate.

Let us consider a constant time delay $\tau_d \in \mathbb{R}^+$ in the input of the system under adaptive control presented in the previous section. This way, we can rewrite the system equations as:

$$\begin{aligned}
\dot{S}(t) &= \lambda - \beta S(t)I(t) - \mu S(t) + u_1(t-\tau_d) \\
\dot{I}(t) &= \beta S(t)I(t) - \gamma I(t) - \delta I(t) - \mu I(t) + u_2(t-\tau_d) \\
\dot{R}(t) &= \gamma I(t) - \mu R(t) + u_3(t-\tau_d) \\
\dot{D}(t) &= \delta I(t)
\end{aligned} \tag{2.23}$$

or, more compactly:

$$\dot{\mathbf{x}}(t) = g(\mathbf{x}(t), \mathbf{u}(t-\tau_d)) \tag{2.24}$$

Our goal is to design a control law to compensate for the delays present in the control inputs. We can do so by using the Predictor-Feedback Control approach. Since our closed-loop system is non-linear and the time delay in the control inputs is a constant variable, we can use the following predictor formula:

$$P(t) = X(t) + \int_{t-\tau_d}^{t} g(P(\theta), U(\theta))d\theta \tag{2.25}$$

where X refers to each component of the state-vector $\mathbf{x}$ and parameter update law, while U refers to the respective control law of each component of the closed-loop system.

By applying the predictor formula to the system states as well as the param-

eter update laws, we get the following functions:

$$
\begin{aligned}
P_S(t) &= S(t) + \int_{t-\tau_d}^{t} (\lambda - \beta P_S(\theta) P_I(\theta) - \mu P_S(\theta) + u_1(\theta)) d\theta \\
P_I(t) &= I(t) + \int_{t-\tau_d}^{t} (\beta P_S(\theta) P_I(\theta) - \gamma P_I(\theta) - \delta P_I(\theta) - \mu P_I(\theta) + u_2(\theta)) d\theta \\
P_R(t) &= R(t) + \int_{t-\tau_d}^{t} (\gamma P_I(\theta) + P_{\hat{\mu}}(\theta) - (\mu + K_3) P_R(\theta)) d\theta \\
P_D(t) &= D(t) + \delta \int_{t-\tau_d}^{t} P_I(\theta) d\theta \\
P_{\hat{\beta}}(t) &= \hat{\beta}(t) + \alpha_1 \int_{t-\tau_d}^{t} P_S(\theta) P_I(\theta) (P_I(\theta) - P_S(\theta)) d\theta \\
P_{\hat{\gamma}}(t) &= \hat{\gamma}(t) + \alpha_2 \int_{t-\tau_d}^{t} P_I(\theta) (P_R(\theta) - P_I(\theta)) d\theta \\
P_{\hat{\delta}}(t) &= \hat{\delta}(t) + \alpha_3 \int_{t-\tau_d}^{t} P_I(\theta) (P_D(\theta) - P_I(\theta)) d\theta \\
P_{\hat{\lambda}}(t) &= \hat{\lambda}(t) + \alpha_4 \int_{t-\tau_d}^{t} P_S(\theta) d\theta \\
P_{\hat{\mu}}(t) &= \hat{\mu}(t) - \alpha_5 \int_{t-\tau_d}^{t} (P_S^2(\theta) + P_I^2(\theta) + P_R^2(\theta)) d\theta
\end{aligned}
\tag{2.26}
$$

By replacing functions P_i, $i \in \{S, I, R, D, \hat{\beta}, \hat{\gamma}, \hat{\delta}, \hat{\lambda}, \hat{\mu}\}$ in our original adaptive controller, we can redefine our control inputs as u_{1p}, u_{2p}, u_{3p}: $\mathbb{R}_0^+ \to \mathbb{R}$ where:

$$
\begin{aligned}
u_{p1}(t) &= P_S(t)(P_{\hat{\beta}}(t) P_I(t) + P_{\hat{\mu}}(t) - K_1) - P_{\hat{\lambda}}(t) \\
u_{p2}(t) &= P_I(t)(P_{\hat{\gamma}}(t) + P_{\hat{\delta}}(t) + P_{\hat{\mu}}(t) - P_{\hat{\beta}}(t) P_S(t) - K_2) \\
&\quad - P_{\hat{\gamma}}(t) P_R(t) - P_{\hat{\delta}}(t) P_D(t) \\
u_{p3}(t) &= P_R(t)(P_{\hat{\mu}}(t) - K_3)
\end{aligned}
\tag{2.27}
$$

As such, we can now define our adaptive predictor-feedback control law vector function $\mathbf{u}_p$: $\mathbb{R}_0^+ \to \mathbb{R}^4$ as:

$$
\mathbf{u}_p(t) = \begin{bmatrix} u_{p1}(t) \\ u_{p2}(t) \\ u_{p3}(t) \\ 0 \end{bmatrix} \tag{2.28}
$$

The above control law ensures that the system has been compensated for any time delays present in it's input, meaning it can be rewritten in the following

form:

$$\dot{\mathbf{x}}(t) = g(\mathbf{x}(t), \mathbf{u}_p(t)) = f(\mathbf{x}(t)) + \mathbf{u}_p(t) \tag{2.29}$$

By taking into account the output vector $\mathbf{y}$ defined in the previous section, the closed-loop system's structure under adaptive predictor-feedback control is presented thoroughly in the block diagram in Figure 2.3:

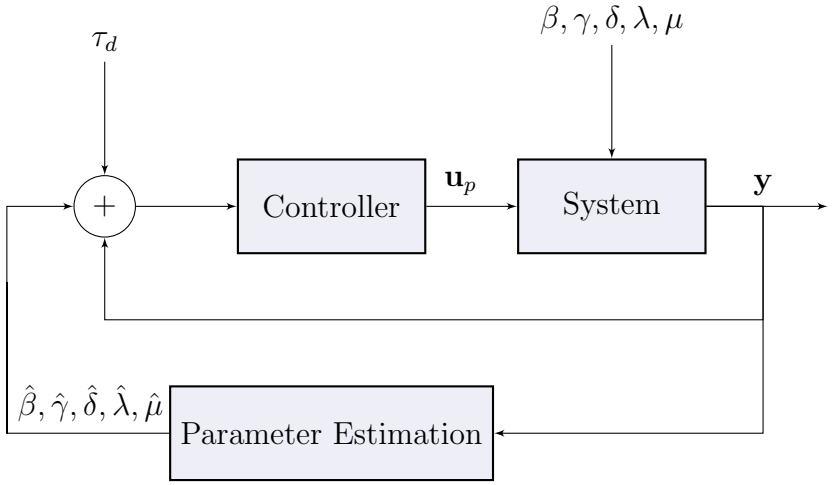

Figure 2.3: The block diagram of the closed-loop $SIRD$ model under adaptive control. Note how the system measurements are used in the calculation of the parameter estimations. The parameter estimations are then used in conjunction with the system measurements in the controller of the system.

Chapter 3

Simulation Setup and Results

3.1 Simulation Setup

3.1.1 Basic Reproduction Number and Parameters

During the controller design process, system parameters β, γ, δ, λ and μ are considered unknown. However, in order to conduct model simulations, these parameters need to be assigned actual values, which our adaptive controller module will try and estimate. The most common approach to achieve this in disease modeling is by using the basic reproduction number R_0.

In epidemiology, the basic reproduction number represents the number of secondary infections produced by each infectious individual among the susceptible population. The exact method of calculating the basic reproduction number varies depending on the parameters used in each epidemiological model. However, it generally involves calculating the ratio at which individuals enter and exit the respective infected state. As such, it is also commonly referred to as the basic reproduction ratio.

One method of determining R_0 is by finding the disease-free equilibrium of the base model presented at (2.4). This can be achieved by assuming that the modeled population is entirely susceptible. No infected individuals are present in the system's population. Consecutively, no recovered or deceased individuals can be present either.

We can compute the disease-free equilibrium of the model by solving the following equation:

$$\dot{S}(t) = \dot{I}(t) = \dot{R}(t) = \dot{D}(t) = 0 \tag{3.1}$$

Using the equations of system (2.4), the disease free equilibrium $\mathbf{x}^*$ is obtained for the following steady-state inputs:

$$\mathbf{x}^*(t) = (S(t), I(t), R(t), D(t)) = (\frac{\lambda}{\mu}, 0, 0, 0) \tag{3.2}$$

As expected, the model's susceptible population is entirely dependent on parameters λ and μ.

We can now determine the behavior of the system around the disease-free equilibrium by examining the eigenvalues which correspond to the roots of the characteristic polynomial at the disease-free equilibrium[31]. The characteristic polynomial can be described using the following equation:

$$p(z) = \det(\mathbf{J}(\mathbf{x}^*(t)) - z\mathbf{I}_{4\times4}) \tag{3.3}$$

where $\mathbf{I}_{4\times4}$ is the identity matrix in $\mathbb{R}^{4\times4}$, $\mathbf{J}$ is the Jacobian matrix of the dynamical system and $z \in \mathbb{C}$: The Jacobian matrix of the system can be computed as follows:

$$\mathbf{J}(\mathbf{x}(t)) = \begin{bmatrix} \frac{\partial \dot{S}(t)}{\partial S} & \frac{\partial \dot{S}(t)}{\partial I} & \frac{\partial \dot{S}(t)}{\partial R} & \frac{\partial \dot{S}(t)}{\partial D} \\ \frac{\partial \dot{I}(t)}{\partial S} & \frac{\partial \dot{I}(t)}{\partial I} & \frac{\partial \dot{I}(t)}{\partial R} & \frac{\partial \dot{I}(t)}{\partial D} \\ \frac{\partial \dot{R}(t)}{\partial S} & \frac{\partial \dot{R}(t)}{\partial I} & \frac{\partial \dot{R}(t)}{\partial R} & \frac{\partial \dot{R}(t)}{\partial D} \\ \frac{\partial \dot{D}(t)}{\partial S} & \frac{\partial \dot{D}(t)}{\partial I} & \frac{\partial \dot{D}(t)}{\partial R} & \frac{\partial \dot{D}(t)}{\partial D} \end{bmatrix} \tag{3.4}$$

By calculating the partial derivatives of system (2.4), we can rewrite (3.5) as follows:

$$\mathbf{J}(\mathbf{x}(t)) = \begin{bmatrix} -\beta I(t) - \mu & -\beta S(t) & 0 & 0 \\ \beta I(t) & \beta S(t) - \gamma - \delta - \mu & 0 & 0 \\ 0 & \gamma & -\mu & 0 \\ 0 & \delta & 0 & 0 \end{bmatrix} \tag{3.5}$$

Substituting the steady-state inputs described in (3.2) directly into the Jacobian matrix, we now obtain:

$$\mathbf{J}(\mathbf{x}^*(t)) = \begin{bmatrix} -\mu & -\beta\frac{\lambda}{\mu} & 0 & 0 \\ 0 & \beta\frac{\lambda}{\mu} - \gamma - \delta - \mu & 0 & 0 \\ 0 & \gamma & -\mu & 0 \\ 0 & \delta & 0 & 0 \end{bmatrix} \tag{3.6}$$

The matrix present in equation (3.3) can now be described as follows:

$$\mathbf{J}(\mathbf{x}^*(t)) - z\mathbf{I}_{4\times 4} = \begin{bmatrix} -\mu - z & -\beta\frac{\lambda}{\mu} & 0 & 0 \\ 0 & \beta\frac{\lambda}{\mu} - \gamma - \delta - \mu - z & 0 & 0 \\ 0 & \gamma & -\mu - z & 0 \\ 0 & \delta & 0 & -z \end{bmatrix} \tag{3.7}$$

Calculating the determinant of the matrix presented in (3.8) yields the characteristic polynomial as follows:

$$p(z) = (z + \mu)(z - \beta\frac{\lambda}{\mu} + \gamma + \delta + \mu)(z + \mu)z \tag{3.8}$$

It is made apparent that the roots of the characteristic polynomial are:

$$(z_1, z_2, z_3, z_4) = (-\mu, \beta\frac{\lambda}{\mu} - \gamma - \delta - \mu, -\mu, 0) \tag{3.9}$$

By taking into account the nontrivial eigenvalues, we know that $z_1, z_3 < 0$ since $\mu \in (0, 1)$. For the equilibrium to be stable, we also require $z_2 < 0$, or, equivalently:

$$\beta\frac{\lambda}{\mu} < \gamma + \delta + \mu \tag{3.10}$$

The basic reproduction number can be obtained from the stability threshold as follows:

$$R_0 = \frac{\beta\lambda}{\mu(\gamma + \delta + \mu)} \tag{3.11}$$

It is made apparent that if $R_0 > 1$, the disease-free equilibrium is unstable, meaning that the number of infected individuals will keep increasing if left uncontrolled. Conversely, if $R_0 < 1$, the disease free equilibrium is stable, meaning that the disease will eventually die out and the population will reach a disease-free state.

We are going to be using Sweden as a point of reference for calibrating our parameter values. The rationale behind this choice lies in the fact that, unlike countries like Greece or Australia, Sweden omitted enforcing strict lockdown policies during the pandemic. Instead, Sweden relied on its population following more elastic mitigation policies. This choice allows us to simulate the $SIRD$ model without control based on real-world parameters and then deduct results by drawing comparisons with the model under the proposed control laws.

We gathered the following information regarding Sweden's population for the year 2020:

- The country's total population amounted to 10,379,295 individuals by the end of the year [32].
- The country's total population increased by 51,706 individuals compared to the end of 2019 [32].
- The total deaths in the country amounted to 90,962. Out of those deaths, 9,815 were contributed to COVID-19 [33].
- The average life expectancy is estimated to 82.36 years [34].

Given the above information and assuming an average recovery period of 10 days as well as a basic reproduction number $R_0 = 1.8$ [35], we can easily calibrate the system parameters. Normalizing per day, the parameter values are presented in Table 3.1:

Name	Parameter Description	Parameter Value	Units
β	Infectious Rate	0.14757	$(\text{day})^{-1}$
γ	Recovery Rate	0.1	$(\text{day})^{-1}$
δ	Mortality Rate (Disease)	0.0000769	$(\text{day})^{-1}$
λ	Birth and Immigration Rate	0.0000315	people/day
μ	Mortality Rate (Natural)	0.0000258	$(\text{day})^{-1}$

Table 3.1: Table of parameter values used in simulations.

3.1.2 Incubation Period and Input Delay

The incubation period of COVID-19 is the time-frame which elapses between an individual's initial exposure to the virus and the point at which they start presenting noticeable symptoms. The incubation period can greatly affect the dynamics of the system in multiple different ways, since symptomatic individuals are less likely to get tested for COVID-19. This not only makes detecting the infected individuals much harder, but it also means that they are less likely to adopt public health policies such as social distancing or quarantine measures.

Since the policies described above are presented as control inputs in the model we propose, it is only reasonable to express the incubation period of the virus as a delay in those inputs. While the incubation period ranges from 1 to 14 days depending on the individual, the average is estimated to be between 5 and 6 days [36]. As such we will be using an input delay of $\tau_d = 5.5$ days in our system simulations and use the adaptive predictor-feedback control module to regulate the delay effect.

3.2 Simulation Results

In this section, we will be individually examining the effects that the final adaptive predictor-feedback module has on output vector $\mathbf{y}$, as defined in (2.22). Simulations are performed on daily increments over the course of a year (365 days), as the uncertain parameters are normalized accordingly.

There are a total of 8 control parameters affecting the behavior of the closed-loop system α_i, $i \in \{1, 2, 3, 4, 5\}$ as well as constants K_j, $j \in \{1, 2, 3\}$. Our goal is to examine the individual effects that each of those parameters have on the system outputs. In order to do so, we will be sliding the value of each of the aforementioned parameters and examining the system outputs, while minimizing the effects of the rest of the parameters. Since all eight of our parameters have been designated during the design process as positive constants, we cannot directly assign their value directly to 0 during the simulation process. As such, we will be assigning them a very small default value of $\epsilon = 1 \cdot 10^{-10}$ which sufficiently approaches zero relative to the total population. Since our system outputs have a co-domain of $[0, 1]$, this is enough to simulate minimal effect of the parameters with a satisfactory error margin.

We will be providing graphs displaying the four states of the closed loop system for different control parameter values, as well as numerical analysis of the simulation results. Specifically, for each iteration, for $X \in \{S, I, R\}$, we will be examining the following indexes:

- X_{avg} (%): The deviation from the average uncontrolled population of compartment X during the course of the simulation.
- $X_{\max}$ (%): The deviation from the uncontrolled maximum value of compartment X during the course of the simulation.
- $X_{\min}$ (%): The deviation from the average uncontrolled maximum value of compartment X during the course of the simulation.
- $t_{X\max}$: The time required (in days) for compartment X to reach its maximum value during the course of the simulation.
- $t_{X\min}$: The time required (in days) for compartment X to reach its minimum value during the course of the simulation.

The average population of each compartment gives us a long-term overview of the system behavior over the course of the simulation, while the maximum and minimum as well as the time to achieve them lets us calibrate the control

parameters to the capabilities of the health-care system.

The time-stamp at which the peak of the infection curve is achieved is critical for the system, as it signifies the period at which the pandemic is at its most dangerous. Thus, during the simulations, the performance of the different control parameters is evaluated based on how they fare against the primary objective of the proposed control strategy - lowering the maximum number of infected individuals at the peak of the simulated pandemic, or "flattening the curve".

The three control parameters that benefited output vector $\mathbf{y}$ the most with regards to the primary objective are adaptation gain a_5, as well as constants K_1 and K_2, with K_2 performing the best, followed up by K_1 and then a_5. The figures of the simulations for each output function, numerical analysis based on the previously provided indexes as well as comments on the simulation data are provided in the following subsections.

3.2.1 Adaptive Predictor-Feedback Controller Simulation Results

- Simulation results for each system state for different values of adaptation gain a_5:

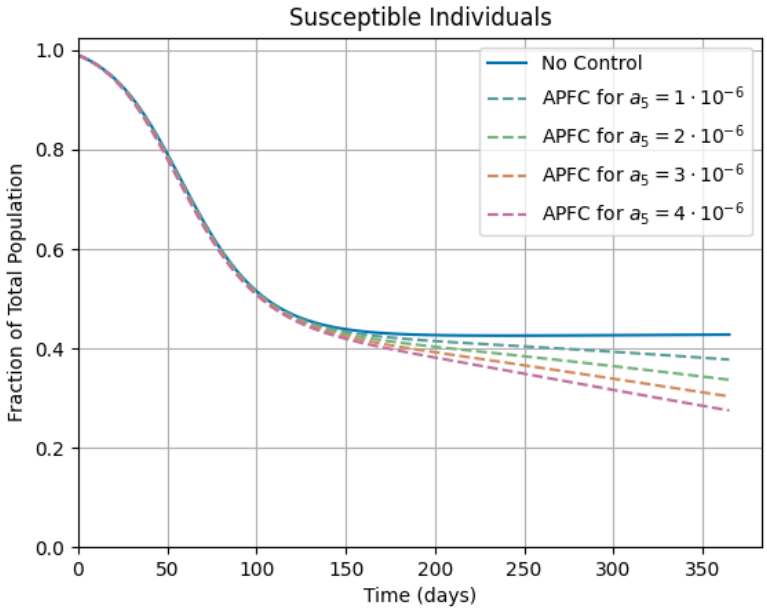

Figure 3.1: Output of function S for different values of adaptation gain a_5.

α_5	S_{avg} (%)	S_{max} (%)	$t_{S\text{max}}$ (days)	S_{min} (%)	$t_{S\text{min}}$ (days)
$1 \cdot 10^{-6}$	-2.93	+0	0	-11.33	365
$2 \cdot 10^{-6}$	-5.51	+0	0	-20.86	365
$3 \cdot 10^{-6}$	-7.81	+0	0	-28.74	365
$4 \cdot 10^{-6}$	-9.91	+0	0	-35.37	365

Table 3.2: Numerical results for the indexes of function I for different values of adaptation gain a_5.

Gradually increasing the value of adaptation gain a_5 decreases the average and minimum number of susceptible individuals. The maximum number of susceptible individuals remains constant and is always achieved at the start of the simulation while the minimum number is always achieved at the end of the simulation for all iterations.

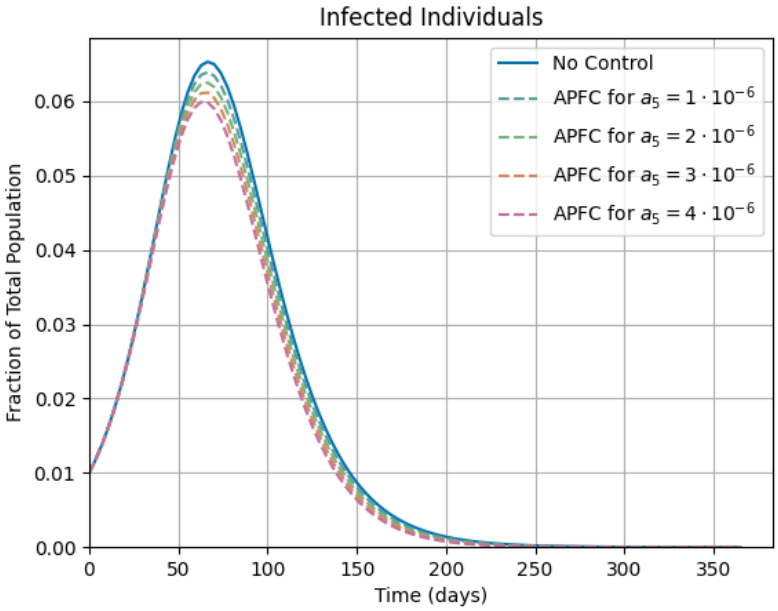

Figure 3.2: Output of function I for different values of adaptation gain a_5.

$\boldsymbol{\alpha_5}$	$\boldsymbol{I_{\text{avg}}}$ (%)	$\boldsymbol{I_{\text{max}}}$ (%)	$\boldsymbol{t_{I\text{max}}}$ (days)	$\boldsymbol{I_{\text{min}}}$ (%)	$\boldsymbol{t_{I\text{min}}}$ (days)
$1 \cdot 10^{-6}$	-2.84	-2.17	66	-0.01	365
$2 \cdot 10^{-6}$	-5.55	-4.29	66	-0.01	365
$3 \cdot 10^{-6}$	-8.12	-6.36	66	-0.02	365
$4 \cdot 10^{-6}$	-10.58	-8.32	62	-0.02	365

Table 3.3: Numerical results for the indexes of function I for different values of adaptation gain a_5.

Gradually increasing the value of adaptation gain a_5 decreases the average, maximum and minimum number of infected individuals. The time required to achieve the maximum marginally decreases while the minimum is always achieved at the end of the simulation for all iterations.

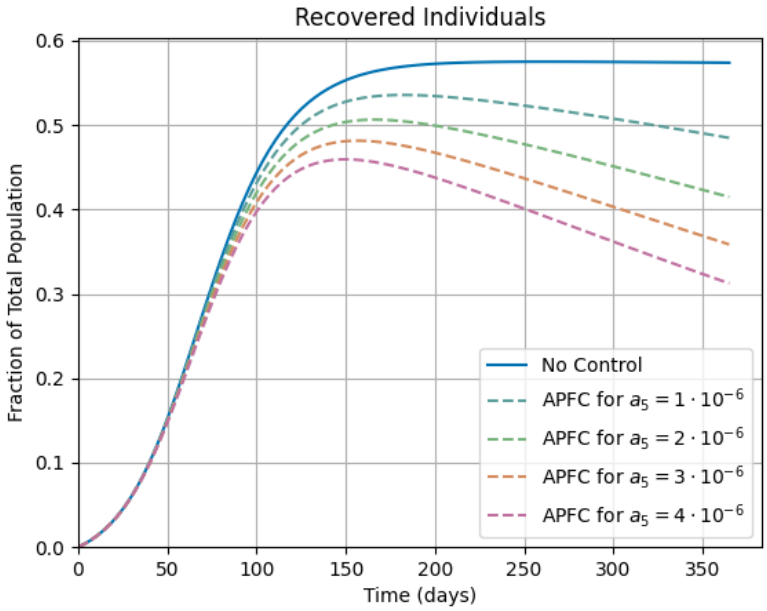

Figure 3.3: Output of function R for different values of adaptation gain a_5.

$\boldsymbol{\alpha_5}$	$\boldsymbol{R_{\text{avg}}}$ (%)	$\boldsymbol{R_{\text{max}}}$ (%)	$\boldsymbol{t_{R\text{max}}}$ (days)	$\boldsymbol{R_{\text{min}}}$ (%)	$\boldsymbol{t_{R\text{min}}}$ (days)
$1 \cdot 10^{-6}$	-7.92	-6.84	180	+0	0
$2 \cdot 10^{-6}$	-14.76	-11.93	165	+0	0
$3 \cdot 10^{-6}$	-20.76	-16.27	154	+0	0
$4 \cdot 10^{-6}$	-26.06	-20.11	151	+0	0

Table 3.4: Numerical results for the indexes of function R for different values of adaptation gain a_5.

Gradually increasing the value of adaptation gain a_5 decreases the average and maximum number of recovered individuals while also decreasing the amount of time required to achieve the maximum. The minimum number of recovered individuals remains constant and always occurs at the start of the simulation for all iterations.

- Simulation results for each system state for different values of cosntant K_1:

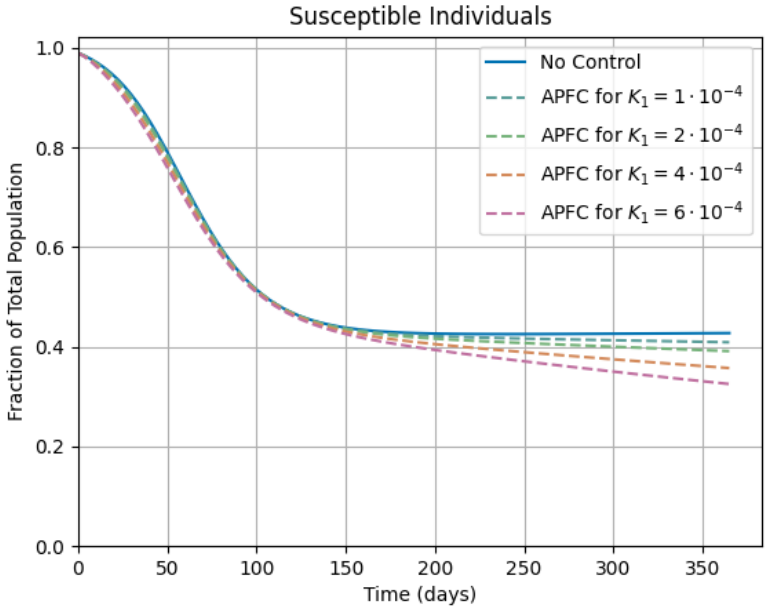

Figure 3.4: Output of function S for different values of constant K_1.

K_1	S_{avg} (%)	S_{max} (%)	t_{Smax} (days)	S_{min} (%)	t_{Smin} (days)
$1 \cdot 10^{-4}$	-1.25	+0	0	-3.84	365
$2 \cdot 10^{-4}$	-2.51	+0	0	-8.03	365
$4 \cdot 10^{-4}$	-5.04	+0	0	-16.02	365
$6 \cdot 10^{-4}$	-7.61	+0	0	-23.5	365

Table 3.5: Numerical results for the indexes of function S for different values of constant K_1.

Gradually increasing the value of constant K_1 decreases the average as well as the minimum number of susceptible individuals. The maximum number of susceptible individuals remains constant and is always achieved at the start of the simulation while the minimum number is always achieved at the end of the simulation for all iterations.

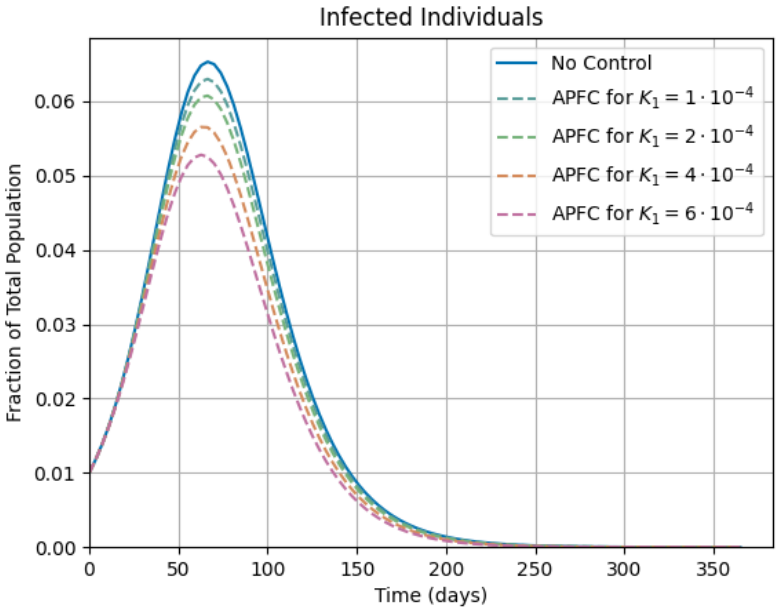

Figure 3.5: Output of function I for different values of constant K_1.

K_1	I_{avg} (%)	I_{max} (%)	t_{Imax} (days)	I_{min} (%)	t_{Imin} (days)
$1 \cdot 10^{-4}$	-3.28	-3.55	66	-0.01	365
$2 \cdot 10^{-4}$	-6.49	-6.99	66	-0.02	365
$4 \cdot 10^{-4}$	-12.69	-13.46	62	-0.03	365
$6 \cdot 10^{-4}$	-18.57	-19.18	62	-0.04	365

Table 3.6: Numerical results for the indexes of function I for different values of constant K_1.

Gradually increasing the value of constant K_1 decreases the average, maximum and minimum number of infected individuals, while marginally decreasing the amount of time required to achieve the maximum. The minimum is always achieved at the end of the simulation for all iterations.

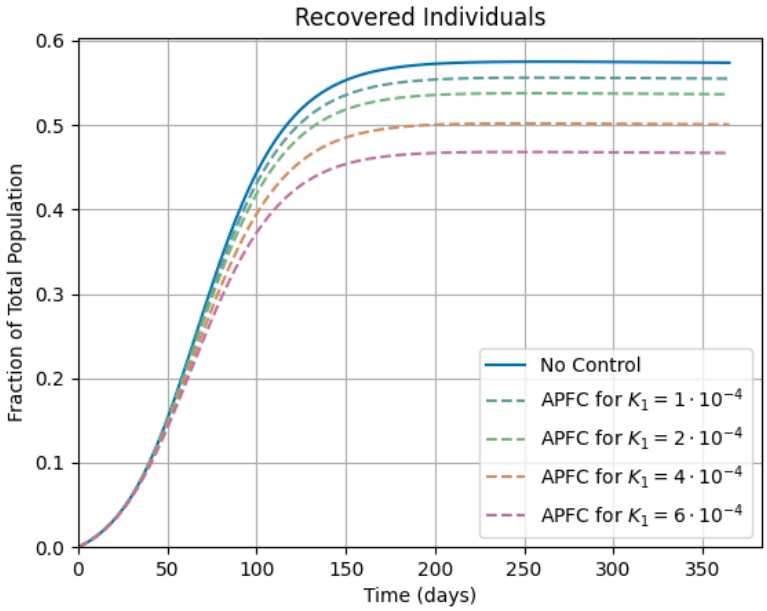

Figure 3.6: Output of function R for different values of constant K_1.

K_1	R_{avg} (%)	R_{max} (%)	t_{Rmax} (days)	R_{min} (%)	t_{Rmin} (days)
$1 \cdot 10^{-4}$	-3.11	-3.28	258	+0	0
$2 \cdot 10^{-4}$	-6.16	-6.51	254	+0	0
$4 \cdot 10^{-4}$	-12.03	-12.71	250	+0	0
$6 \cdot 10^{-4}$	-17.59	-18.59	243	+0	0

Table 3.7: Numerical results for the indexes of function R for different values of constant K_1.

Gradually increasing the value of constant K_1 decreases the average and maximum number of recovered individuals while also decreasing the amount of time required to achieve the maximum. The minimum number of recovered individuals remains constant and is always present at the start of the simulation for all iterations.

- Simulation results for each system state for different values of constant K_2:

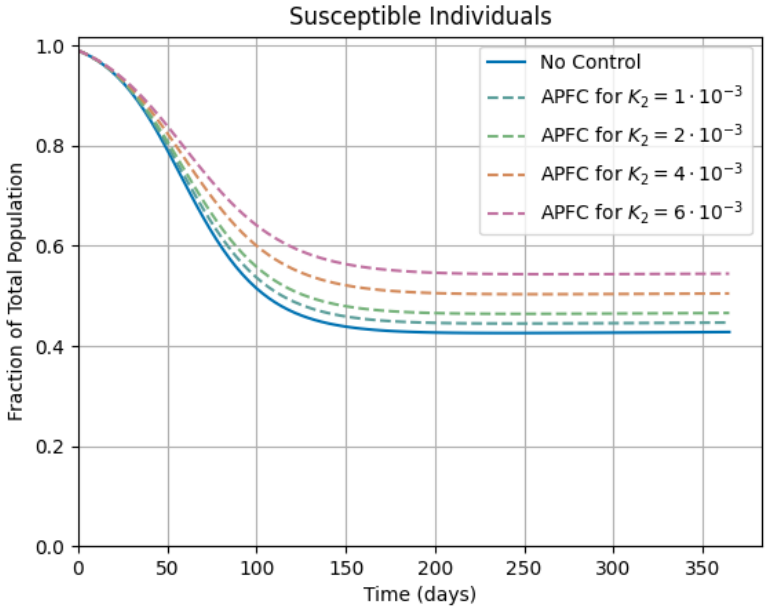

Figure 3.7: Output of function S for different values of constant K_2.

K_2	S_{avg} (%)	S_{max} (%)	t_{Smax} (days)	S_{min} (%)	t_{Smin} (days)
$1 \cdot 10^{-3}$	+3.17	+0	0	+4.48	243
$2 \cdot 10^{-3}$	+6.36	+0	0	+9.01	247
$4 \cdot 10^{-3}$	+12.78	+0	0	+18.23	258
$6 \cdot 10^{-3}$	+19.21	+0	0	+27.59	260

Table 3.8: Numerical results for the indexes of function S for different values of constant K_2.

Gradually increasing the value of constant K_2 increases the average and minimum number of susceptible individuals while also increasing the amount of time required to achieve the minimum. The maximum number of susceptible individuals remains constant and always occurs at the start of the simulation for all iterations.

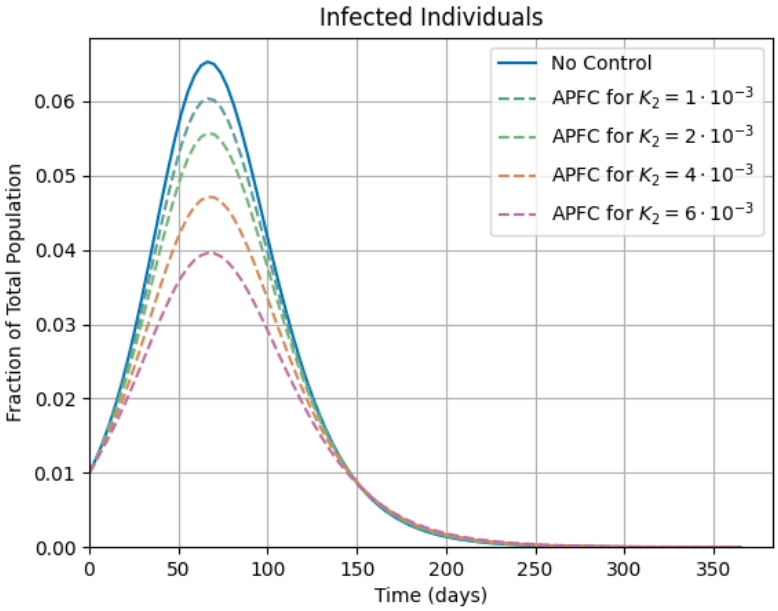

Figure 3.8: Output of function I for different values of constant K_2.

K_2	I_{avg} (%)	I_{max} (%)	t_{Imax} (days)	I_{min} (%)	t_{Imin} (days)
$1 \cdot 10^{-3}$	-5.16	-7.56	66	+0.01	365
$2 \cdot 10^{-3}$	-10.17	-14.73	66	+0.01	365
$4 \cdot 10^{-3}$	-19.72	-27.85	66	+0.02	365
$6 \cdot 10^{-3}$	-28.71	-39.41	66	+0.02	365

Table 3.9: Numerical results for the indexes of function I for different values of constant K_2.

Gradually increasing the value of constant K_2 decreases the average and maximum number of infected individuals while increasing the minimum number of infected individuals. The maximum and minimum are always achieved at a constant amount of time, with the latter occurring at the end of the simulation for all iterations.

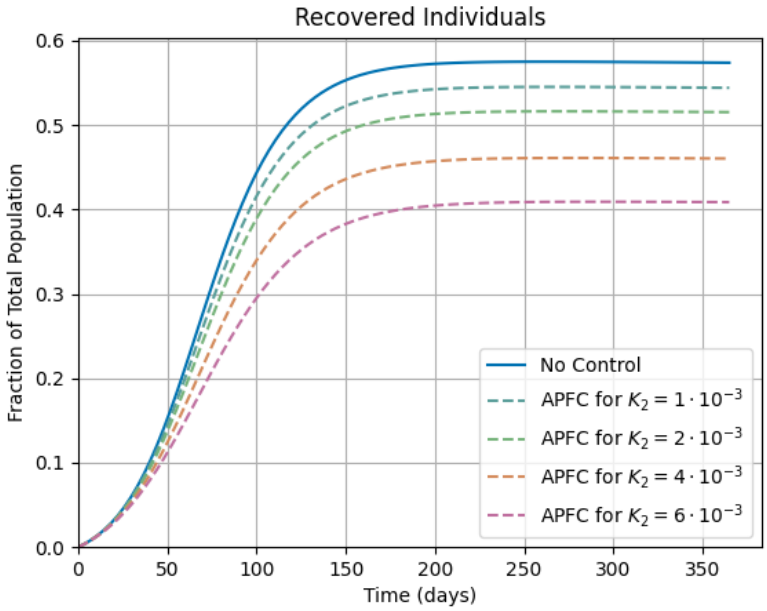

Figure 3.9: Output of function R for different values of constant K_2.

K_2	R_{avg} (%)	R_{max} (%)	t_{Rmax} (days)	R_{min} (%)	t_{Rmin} (days)
$1 \cdot 10^{-3}$	-5.38	-5.19	265	+0	0
$2 \cdot 10^{-3}$	-10.58	-10.22	269	+0	0
$4 \cdot 10^{-3}$	-20.49	-19.82	280	+0	0
$6 \cdot 10^{-3}$	-30.41	-28.84	291	+0	0

Table 3.10: Numerical results for the indexes of function R for different values of constant K_2.

Gradually increasing the value of constant K_2 decreases the average and maximum number of recovered individuals while decreasing the amount of time required to achieve the maximum. The minimum number of recovered individuals remains constant and is always achieved at the start of the simulation.

3.2.2 Simulation Result Summary and Discussion

The simulations and evaluation of the key indexes in the previous sub-section yielded interesting insights on how each one of the parameters used in the proposed control module impact the output of the system. First, we noted that a single parameter shift can impact all three output functions at once. For example, increasing the value of constant K_2 increases the average number of susceptible individuals while decreasing the average number of infected and recovered individuals. This is in contrast with constant K_1 which decreases the average outputs across all three functions, albeit not in a uniform manner.

Simulations also indicated that our control parameters vary highly in terms of sensitivity, both with respect to one another and with respect to each compartment indexes. For example, constants $K_2 = 2 \cdot 10^{-3}$ and adaptation gain $a_5 = 4 \cdot 10^{-6}$ yield a -10.17% and -10.58% change in the average number of infected individuals respectively. The effect on the output is very similar in both cases, even though the two control parameters differ by three orders of magnitude. As such, we can deduct that the adaptation gain a_5 is much more sensitive than constant K_2 with respect to this specific key index. However, this sensitivity is not uniform across indexes, since those two parameters yield entirely different results with respect to the average number of susceptible individuals, with a change of +6.36% and -9.91% respectively.

Next, we examined how each parameter shift impacted the extreme values of the system outputs. We noted that the maximum and minimum outputs of each compartment followed a similar pattern of fluctuation to the average number of individuals for the respective compartment. For example, if a parameter shift caused the average number of infected individuals to decrease, it also meant that the maximum number of infected individuals also decreased.

We also evaluated how each control parameter shift impacted the time required to achieve the maximum and minimum value of each compartment. We noticed that the maximum number of susceptible individuals was always achieved at the start of the simulation. The maximum number of recovered individuals fluctuated greatly upon parameter shifts, while the maximum number of infected individuals was always achieved around the 2-month time-stamp, thus marking the most contagious period of the phenomenon. Respectively the minimum number of recovered and deceased individuals was always achieved at the start of the simulation, with the minimum number of infected individuals generally occurring at the end of the time horizon.

The minimum number of susceptible individuals was mostly affected by the difference in control parameter values.

During simulations, we noticed a reduced output of recovered individuals for all three cases of control parameters. This is directly correlated with the effect of the control law in the I compartment, as fewer infected individuals directly translates to fewer individuals in need of recovery, hence explaining the reduced output of the R compartment.

When adjusting the control parameters, we need to take into account constrains provided by the given population and health-care system. For example, it is generally preferred increasing the value of a control parameter such as K_2 that increases the number of susceptible individuals while decreasing the number of infected individuals as this translates to fewer healthy individuals being quarantined and thus able to actively participate in socio-economical activities. Respectively, a health-care system with a high number of available ICUs can afford treating a lot more individuals at the early stages of the pandemic. As such we can adjust our control parameter magnitude to achieve a higher maximum number of recovered individuals at a brief time-frame.

The results highlight that selecting the correct parameter values for each case is an new optimization problem in itself. This can be further expanded upon given the linear nature of the controller or by using specific maximum output values as reference.

Chapter 4

Conclusions and Future Work

In this thesis, we briefly discussed the global impact of the COVID-19 pandemic, as well as the importance of mathematical epidemiology in combating such events. After conducting an overview of the various mathematical tools available, we focused on nonlinear systems, presenting an $SIRD$ system in order to emulate the behavior of the pandemic. Two key concerns were raised at this stage - the uncertain behavior of the system parameters such as infection, recovery and mortality rates within the system dynamics, as well as the incubation period of the virus, which makes detecting infected individuals a challenging task.

In order to address those factors, we introduced two different control modules, focusing on emulating the effects of lockdowns or similar control policies. We presented an adaptive control module in order to address the uncertain behavior of the system parameters and ensure stability, while we also introduced a predictor-feedback control module in order to address delay in the system inputs caused by the incubation period of the virus.

After calibrating the system parameters based on real data from the COVID-19 pandemic breakout in Sweden, we thoroughly examined the behavior of the system outputs over the course of a year under adaptive predictor-feedback control. We used different values for the adaptation and the constants that were derived from the theoretical analysis of the model and compared their effect on the behavior of the system.

Upon evaluating the simulations, we compared the outputs of the system using the final control module, for multiple different adaptation gain and constant values. It is evident that each of those parameters has a different impact on each system compartment. This allows us to choose a set

of parameters that fits the conditions that our health-care system needs to match. For example, the average age of our target population might be relatively low, making them much less likely to die from the disease when infected. In this case, we might want to pick a specific combination of adaptation gains and constants that focus on minimizing the population of the deceased compartment, with the downside of increasing the population of the infected compartment, etc.

The field of nonlinear system control is of particular importance to mathematical epidemiology. It contains a plethora of different tools and approaches, while it is constantly being expanded upon as new research emerges. Alternative approaches to the adaptive control problem include the use of model-reference adaptive control (MRAC) modules [37], which use a reference system in order to adjust the behavior of uncertain parameters in real time. The reference system could be calibrated in order to fit the characteristics and necessities that different health-care systems might introduce.

The use of predictor-feedback controllers could also be further expanded upon using different state-based controllers in order to describe more complex system dynamics related to state-dependent input-delays [38]. These could include the re-introduction of infected individuals to the pool of susceptible individuals after temporary immunity has worn off, simulating the time patients spend in the ICU, implementing vaccination policies, etc.

Appendix A - Simulation Code

The model simulations were conducted using Python 3.9. The simulation code includes the following python modules:

- The **main.py** module, which includes the driver code used to plot the various graphs presented in Chapter 3.
- The **models.py** module, which includes various methods simulating the model behavior without control, under adaptive control and under adaptive predictor-feedback control respectively.

The following methods were imported in the **main.py** module from existing Python libraries in order to plot the various graphs used in the thesis:

- **linspace** from the **numpy** library was used in order to create the time horizon for the simulations.
- **odeint** from the **scipy.integrate** library was used in order to simulate the differential equations of the system.
- Various methods from the **matplotlib.pyplot** library, such as **plot** and **show**, were used in order to plot the graphs for the simulations.

The code for the main.py module is listed below:

```
import numpy as np
import scipy.integrate as spi
import matplotlib.pyplot as plt
from models import *

# Driver code:
if __name__ == "__main__":

    # Initializing the simulation time horizon
    # over the course of a year:
    t_min = 0
    t_max = 365
    t_spacing = 100
    t_values = np.linspace(t_min, t_max, t_spacing)

    # Initializing the initial conditions for the various
    # systems:
    init_con_sird = [0.99, 0.01, 0, 0]
    init_con_sird_ac = [0.99, 0.01, 0, 0, 0, 0, 0, 0, 0]
    init_con_sird_apfc = [0.99, 0.01, 0, 0, 0, 0, 0, 0, 0]

    # Initializing the uncertain parameters:
    # beta, gamma, delta, lambda, mu
    unc_par = [0.314, 0.1, 0.001, 0.00792, 0.01224]

    # Initializing the adaptation gains for
    # the adaptive controllers:
    adp_gains = [0.0001, 0.00001, 0.0001, 0.00001, 0.00001]

    # Initializing the diffusion coefficients for
    # the adaptive controllers:
    cons = [0.0001, 0.0001]

    # Initializing the input delay in terms of days:
    t_d = 5.5

    # Initializing the integration step:
    dt = 0.00001

    # Initializing the number of integration steps:
    N = 1000

    # Simulating the model without control:
    sim_sird = spi.odeint(sird, init_con_sird, t_values,
                          args=(unc_par,))
```

```
# Simulating the model with adaptive control:
sim_sird_ac = spi.odeint(sird_ac, init_con_sird_ac,
                         t_values, args=(unc_par,
                         adp_gains, cons))

# Simulating the model with adaptive
# predictor-feedback control:
sim_sird_apfc = spi.odeint(sird_apfc, init_con_sird_apfc,
                           t_values, args=(unc_par,
                           adp_gains, cons, t_d,
                           dt, N))

# Plotting the graph of susceptible individuals:
plt.figure(1)
plt.plot(t_values, sim_sird[:, 0], label='No Control',
         linestyle='solid', color='#0072B2')
plt.plot(t_values, sim_sird_ac[:, 0], label='AC',
         linestyle='dashed', color='#009E73')
plt.plot(t_values, sim_sird_apfc[:, 0], label='APFC',
         linestyle='dashed', color='#009E73')
plt.xlim(0)
plt.ylim(0)
plt.xlabel('Time (days)')
plt.ylabel('Fraction of Total Population')
plt.title('Susceptible Individuals')
plt.legend(loc='best')
plt.legend()
plt.grid(True)

# Plotting the graph of infected individuals:
plt.figure(2)
plt.plot(t_values, sim_sird[:, 1], label='No Control',
         linestyle='solid', color='#0072B2')
plt.plot(t_values, sim_sird_ac[:, 1], label='AC',
         linestyle='dashed', color='#009E73')
plt.plot(t_values, sim_sird_apfc[:, 1], label='APFC',
         linestyle='dashed', color='#009E73')
plt.xlim(0)
plt.ylim(0)
plt.xlabel('Time (days)')
plt.ylabel('Fraction of Total Population')
plt.title('Infected Individuals')
plt.legend(loc='best')
plt.legend()
plt.grid(True)
```

```
# Plotting the graph of recovered individuals:
plt.figure(3)
plt.plot(t_values, sim_sird[:, 2], label='No Control',
         linestyle='solid', color='#0072B2')
plt.plot(t_values, sim_sird_ac[:, 2], label='AC',
         linestyle='dashed', color='#009E73')
plt.plot(t_values, sim_sird_apfc[:, 2], label='APFC',
         linestyle='dashed', color='#009E73')
plt.xlim(0)
plt.ylim(0)
plt.xlabel('Time (days)')
plt.ylabel('Fraction of Total Population')
plt.title('Recovered Individuals')
plt.legend(loc='best')
plt.legend()
plt.grid(True)

# Plotting the graph of deceased individuals:
plt.figure(4)
plt.plot(t_values, sim_sird[:, 3], label='No Control',
         linestyle='solid', color='#0072B2')
plt.plot(t_values, sim_sird_ac[:, 3], label='AC',
         linestyle='dashed', color='#009E73')
plt.plot(t_values, sim_sird_apfc[:, 3], label='APFC',
         linestyle='dashed', color='#009E73')
plt.xlim(0)
plt.ylim(0)
plt.xlabel('Time (days)')
plt.ylabel('Fraction of Total Population')
plt.title('Deceased Individuals')
plt.legend(loc='best')
plt.legend()
plt.grid(True)

plt.show(block=True)
```

The code for the **models.py** module is listed below:

```
# Method that returns the open-loop SIRD model without control:
def sird(x, t, unc_par):

    # Decomposing the state-vector
    S, I, R, D = x

    # Decomposing the uncertain parameter vector:
    b, c, d, l, m = unc_par

    # Defining the system equations:
    S_dot = l - b * S * I - m * S
    I_dot = b * S * I - c * I - d * I - m * I
    R_dot = c * I - m * R
    D_dot = d * I

    # Re-composing the system of equations and returning:
    return [S_dot, I_dot, R_dot, D_dot]


# Method that returns the closed-loop SIRD model
# with adaptive control:
def sird_ac(x, t, unc_par, adp_gains, cons):

    # Decomposing the state-vector:
    S, I, R, D, b_hat, c_hat, d_hat, l_hat, m_hat = x

    # Decomposing the uncertain parameter vector:
    b, c, d, l, m = unc_par

    # Decomposing the adaptation gain vector:
    a_1, a_2, a_3, a_4, a_5 = adp_gains

    # Decomposing the diffusion coefficient vector:
    K_1, K_2, K_3 = cons

    # Defining the adaptive control laws:
    u_1 = S * (b_hat * I + m_hat - K_1) - l_hat
    u_2 = I * (c_hat + d_hat + m_hat - b_hat * S - K_2)\
        - c_hat * R - d_hat * D
    u_3 = R * (m_hat - K_3)

    # Defining the system equations:
    S_dot = l - b * S * I - m * S + u_1
    I_dot = b * S * I - c * I - d * I - m * I + u_2
    R_dot = c * I - m * R
    D_dot = d * I

    # Defining the parameter update laws:
```

```
    b_hat_dot = a_1 * S * I * (I - S)
    c_hat_dot = a_2 * I * (R - I)
    d_hat_dot = a_3 * I * (D - I)
    l_hat_dot = a_4 * S
    m_hat_dot = - a_5 * (S ** 2 + I ** 2 + R ** 2)

    # Re-composing the system of equations and returning:
    return [S_dot, I_dot, R_dot, D_dot, b_hat_dot, c_hat_dot,
            d_hat_dot, l_hat_dot, m_hat_dot]


# Method that returns the closed-loop SIRD model
# with adaptive predictor-feedback control:
def sird_apfc(x, t, unc_par, adp_gains, cons, t_d, dt, steps):

    # Decomposing the state-vector:
    S, I, R, D, b_hat, c_hat, d_hat, l_hat, m_hat = x

    # Decomposing the uncertain parameter vector:
    b, c, d, l, m = unc_par

    # Decomposing the adaptation gain vector:
    a_1, a_2, a_3, a_4, a_5 = adp_gains

    # Decomposing the diffusion coefficient vector:
    K_1, K_2, K_3 = cons

    # Defining the adaptive control laws:
    u_1 = S * (b_hat * I + m_hat - K_1) - l_hat
    u_2 = I * (c_hat + d_hat + m_hat - b_hat * S - K_2) \
        - c_hat * R - d_hat * D
    u_3 = R * (m_hat - K_3)

    # Defining the parameter update laws:
    b_hat_dot = a_1 * S * I * (I - S)
    c_hat_dot = a_2 * I * (R - I)
    d_hat_dot = a_3 * I * (D - I)
    l_hat_dot = a_4 * S
    m_hat_dot = - a_5 * (S ** 2 + I ** 2 + R ** 2)

    # Calculating the predictor feedback components
    # for t - t_d < 0:
    P_S = S
    P_I = I
    P_R = R
    P_D = D
    P_b_hat = b_hat
    P_c_hat = c_hat
    P_d_hat = d_hat
```

```
P_l_hat = l_hat
P_m_hat = m_hat

# Calculating the predictor-feedback law components
# for t - t_d >= 0:
if t - t_d >= 0:

    # Calculating the integral component:
    for step in range(steps):
        P_S += (l - b * P_S * P_I - m * P_S + u_1) * dt
        P_I += (b * P_S * P_I - c * P_I - d * P_I
                - m * P_I + u_2) * dt
        P_R += (c * P_I - m * P_R + u_3) * dt
        P_D += d * P_I * dt
        P_b_hat += (a_1 * P_S * P_I * (P_I - P_S)) * dt
        P_c_hat += (a_2 * (P_I * (P_R - P_I))) * dt
        P_d_hat += (a_3 * P_I * (P_D - P_I)) * dt
        P_l_hat += (a_4 * P_S) * dt
        P_m_hat += (-a_5 * (P_S ** 2 + P_I ** 2
                            + P_R ** 2)) * dt

    # Assembling the integral and non-integral component:
    P_S += S
    P_I += I
    P_R += R
    P_D += D
    P_b_hat += b_hat
    P_c_hat += c_hat
    P_d_hat += d_hat
    P_l_hat += l_hat
    P_m_hat += m_hat

# Defining the adaptive-predictor feedback control laws:
u_p1 = P_S * (P_b_hat * P_I + P_m_hat - K_1) - P_l_hat
u_p2 = P_I * (P_c_hat + P_d_hat + P_m_hat - P_b_hat * P_S \
             - K_2) - P_c_hat * P_R - P_d_hat * P_D
u_p3 = P_R * (P_m_hat - K_3)

# Defining the system equations:
S_dot = l - b * S * I - m * S + u_p1
I_dot = b * S * I - c * I - d * I - m * I + u_p2
R_dot = c * I - m * R + u_p3
D_dot = d * I

# Re-composing the system of equations and returning:
return [S_dot, I_dot, R_dot, D_dot, b_hat_dot, c_hat_dot,
        d_hat_dot, l_hat_dot, m_hat_dot]
```

References

1. **David E. Bloom, David Canning, Jaypee Sevilla**. "The Effect of Health on Economic Growth: A Production Function Approach". In: *World Development*, Vol. 32 No. 1 (2004) (cit. on pp. 9-11). DOI: 10.1016/j.worlddev.2003.07.002

2. **Hassan Abdi Hussein**. "Brief Review on Ebola Virus Disease and One Health Approach". In: *Heliyon*, Vol. 9 No. 8 (2023) (cit. on pp. 2, 3). DOI: 10.1016/j.heliyon.2023.e19036

3. **James D. Cherry, Paul Krogstad**. "SARS, The First Pandemic of the 21st Century". In: *Emerging Infectious Diseases*, Vol. 10 No. 11 (2004) (cit. on p. 1). DOI: 10.3201/eid1011.040797_02

4. **Anshika Sharma, Isra Ahmad Farouk, Sunil Kumar Lal**. "COVID-19: A Review on the Novel Coronavirus Disease - Evolution, Transmission, Detection, Control and Prevention". In: *Viruses*, Vol. 13 No. 2 (2021) (cit. on pp. 3-4). DOI: 10.3390/v13020202

5. **Neeltje van Doremalen et al.** "Aerosol and Surface Stability of SARS-CoV-2 as Compared with SARS-COV-1". In: *New England Journal of Medicine*, Vol. 382 No. 16 (2020) (cit. on pp. 1-3). DOI: 10.1056/NEJMc2004973

6. **Yousef Alimohamadi et al.** "Determine the Most Common Clinical Symptoms in COVID-19 Patients: A Systematic Review and Meta-Analysis". In: *Journal of Preventitive Medicine and Hygiene*, Vol. 61 No. 3 (2020) (cit. on pp. 2-6). DOI: 10.15167/2421-4248/jpmh2020.61.3.1530

7. **Kelly Wolfe, Miroslav Sirota, Alasdair D.F. Clarke**. "Age Differences in COVID-19, Risk-Taking and the Relationship with Risk Attitude and Numerical Ability". In: *The Royal Society Publishing* Vol. 8 No. 9 (2021) (cit. on p. 3). DOI: 10.1098/rsos.201445

8. **Marina Treskova-Scharzback et al.** "Preexisting Health Conditions and Severe COVID-19 Outcomes: An Umbrella Review Approach and Meta-Analysis of Global Evidence". In: *BMC Medicine* Vol. 21 No. 1 (2021). (cit. on pp. 5-10) DOI: 10.1186/s12916-021-02058-6

9. **World Health Organization**. *WHO-convened Global Study of Origins of SARS-CoV-2: China Part* (2021) (cit. on pp. 7, 42) URL: https://www.who.int/publications/i/item/who-convened-global-study-of-origins-of-sars-cov-2-china-part

10. **World Health Organization**. *Coronavirus Disease (COVID-19) Pandemic*. URL: \https://www.who.int/europe/emergencies/situations/covid-19

11. **Jacques Reis et al.** "COVID-19: Early Cases and Disease Spread". In: *Annals of Global Health*, Vol. 87 No. 1 (2022) (cit. on p. 7). DOI: 10.5334/aogh.3776

12. **Dimitrios Moris, Dimitrios Schizas**. "Lockdown During COVID-19: The Greek Success". In: *In Vivo*, Vol. 32 No. 3 (2020) (cit. on pp. 1695-1698). DOI: 10.21873/invivo.11963

13. **Marlon Fritz, Thomas Gries, Margarete Redlin**. "The Effectiveness of Vaccination, Testing and Lockdown Strategies Against COVID-19". In: *International Journal of Health, Economics and Management*, Vol. 23 No. 4 (2023) (cit. on p. 602). DOI: 10.1007/s10754-023-09352-1

14. **Ulrich Kalinke et al.** "Clinical Development and Approval of COVID-19 Vaccines". In: *Taylor & Francis Online*, Vol. 21, No. 5 (2022) (cit. on p. 4). DOI: 10.1080/14760584.2022.2042257

15. **Aminul Islam** "A Review of SARS-CoV-2 Variants and Vaccines: Viral Properties, Mutations, Vaccine Efficacy and Safety". In: *Infectious Medicine (Beijing)*, Vol. 2 No. 4 (2023) (cit. on p. 256). DOI: 10.1016/j.imj.2023.08.005

16. **World Health Organization**. *WHO COVID-19 Dashboard*. URL: https://data.who.int/dashboards/covid19/deaths

17. **Nicolas Bacaër**. *A Short History of Mathematical Population Dynamics* (2011) (cit. on pp. 21-22)

18. **Fred Brauer**. "Mathematical Epidemiology: Past, Present and Future". In: *Infectious Disease Modelling*, Vol. 2 No. 1 (2017) (cit. on pp. 115-116). DOI: 10.1016/j.idm.2017.02.001

19. **Fred Brauer, Pauline van den Driessche, Jianhong Wu**. *Mathematical Epidemiology* (2008) (cit. on pp. 25-26)

20. **Dave Osthus et al.** "Forecasting Seasonal Influenza with a State-Space SIR Model". In: *The Annals of Applied Statistics*, Vol. 11 No. 1 (2017) (cit. on p. 3). DOI: 10.1214/16-AOAS1000

21. **Ian Cooper, Argha Mondal, Chris G. Antonopoulos** "A SIR Model Assumption for the Spread of COVID-19 in Different Communities". In: *Chaos, Solitons & Fractals*, Vol. 139 (2020) (cit. on p. 2). DOI: 10.1016/j.chaos.2020.110057

22. **Abdul Kuddus et al.** "A Modified SIR Model to Study on Physical Behaviour Among Smallpox Infective Population in Bangladesh". In: *American Journal of Mathematics and Statistics*, Vol. 4 No. 5 (2014) (cit. on p. 233). DOI: 10.5923/j.ajms.20140405.04

23. **Sylvie Diane Djiomba Njankou, Farai Nyabadza** "Modeling the Role of Human Behaviour in Ebola Virus Disease (EVD) Transmission Dynamics". In: *Computational and Mathematical Methods in Medicine*, Vol. 4 (2023) (cit. on pp. 3-4). DOI: 10.1155/2022/4150043

24. **Sakshi Shringi, et al.** "Modified SIRD Model for COVID-19 Spread Prediction for Northern and Southern States of India". In: *Chaos, Solitons and Fractals*, Vol. 148 (2021) (cit. on pp. 3-5). DOI: 10.1016/j.chaos.2021.111039

25. **Simeon Adeyemo, Adekunle Sangotola, Olga Korosteleva** "Transmission Dynamics of Tuberculosis-HIV Co-Infection in South Africa". In: *Epidemiologia*, Vol. 4 (2023) (cit. on pp. 411-415). DOI: 10.3390/epidemiologia4040036

26. **Ramesh Chandra Poonia, et al.** "An Enhanced SEIR Model for Prediction of COVID-19 with Vaccination Effect". In: *Life*, Vol. 12 (2022) (cit. on pp. 655-657). DOI: 10.3390/life12050647

27. **Keith R. Bisset, et al.** "Agent-Based Computational Epidemiological Modeling". In: *J. Indian Inst. Sci.*, Vol. 101 (2021) (cit. on p. 304). DOI: 10.1007/s41745-021-00260-2

28. **Christian Nitzsche, Stefan Simm** "Agent-Based Modeling to Estimate the Impact of Lockdown Scenarios and Events on a Pandemic Exemplified on SARS-CoV-2". In: *Scientific Reports*, Vol. 14 (2024) (cit. on pp. 1-2). DOI: 10.1038/s41598-024-63795-1

29. **Hazhir Rahmandad, John Sterman** "Heterogeneity and Network Structure in the Dynamics of Diffusion: Comparing Agent-Based and Differential Equation Models". In: *Management Science*, Vol. 54 No. 5 (2008) (cit. on pp. 2-3). DOI: 10.1287/mnsc.1070.0787

30. **Fred Brauer, Pauline van den Driessche, Jianhong Wu**. *Mathematical Epidemiology* (2008) (cit. on p. 47)

31. **Marwan Al-Raeei** "The basic reproduction number of the new coronavirus pandemic with mortality for India, the Syrian Arab Republic, the United States, Yemen, China, France, Nigeria and Russia with different rate of cases". In: *Clinical Epidemiology and Global Health*, Vol. 9 No. 1 (2021) (cit. on p. 148). DOI: 10.1016/j.cegh.2020.08.005

32. **Statistikmyndigheten SCB**. *Sweden's Population in 2020 - Population Changes*. URL: https://www.scb.se/en/finding-statistics/statistics-by-subject-area/population/population-composition/population-statistics/pong/statistical-news/swedens-population-2020--population-changes/

33. **Johns Hopkins University**. *Sweden Data Timeline*. URL: https://coronavirus.jhu.edu/region/sweden

34. **Statistikmyndigheten SCB**. *Remaining Average Life Expectancy at Birth and Age 65 by Sex 1970-2023 and Projection 2024-2070*. URL: https://www.scb.se/en/finding-statistics/statistics-by-subject-area/population/population-projections/population-projections/pong/tables-and-graphs/life-expectancy-at-birth-and-age-65-by-sex-and-projection/

35. **Kevin Linka, et al.** "The Reproduction Number of COVID-19 and Its Correlation with Public Health Interventions". In: *COVID-19 SARS-CoV-2 preprints from medRxiv and bioRxiv*, Vol. 101 (2021) (cit. on p. 5). DOI: 10.1007/s00466-020-01880-8

36. **World Health Organization**. *Coronavirus disease 2019 (COVID-19) Situation Report - 73* (2020) (cit. on p. 2) URL: https://www.who.int/docs/default-source/coronaviruse/situation-reports/20200402-sitrep-73-covid-19.pdf

37. **Jean-Jacques E. Slotine, Weiping Li**. *Applied Nonlinear Control* (1990) (cit. on p. 315)

38. **Nikolaos Bekiaris-Liberis, Miroslav Krstic** "Robustness of Nonlinear Predictor Feedback Laws to Time- and State-Dependent Delay Perturbations". In: *Automatica*, Vol. 49 (2013) (cit. on p. 1577). DOI: 10.1016/j.automatica.2013.02.050